Utilization of Secondary Electron Emission Principle in Calorimeter Active Media

B. Bilki[1,2,3,*], *K.*Dilsiz[4,], *H.*Ogul[5,], *Y.*Onel[2,], *K.K.*Sahbaz[3,6,], *D.*Southwick[2,], *E.*Tiras[7,], *M.*Tosun[8,], *J.*Wetzel[2,9,], and *D.*Winn[10,]

[1]Istanbul Beykent University, Istanbul, Turkey
[2]University of Iowa, Iowa City, IA, USA
[3]Turkish Accelerator and Radiation Laboratory, Ankara, Turkey
[4]Bingol University, Bingol, Turkey
[5]Sinop University, Sinop, Turkey
[6]Ankara University, Ankara, Turkey
[7]Erciyes University, Kayseri, Turkey
[8]Istinye University, Istanbul, Turkey
[9]Coe College, Cedar Rapids, IA, USA
[10]Fairfield University, Fairfield, CT, USA

Abstract. Secondary electron emission is the primary signal formation and/or amplification technique utilized in accelerator beam monitors and photomultiplier tubes where incident energetic particles cause ejection of additional electrons from a secondary emission surface. The materials employed as surfaces for secondary electron emission have demonstrated exceptional resistance to radiation, making them suitable for serving as the active media in radiation-hard calorimeters. With this motivation, we developed dedicated secondary electron emission sensor modules, tested them with particle beams and developed Monte Carlo simulations to predict the performance of large-scale calorimeters. Here, the details of the sensor modules and the results of the beam tests and simulations will be discussed.
Recently, we have applied high secondary emission yield materials, Al_2O_3 and TiO_2, as surface coatings on the anode plates of one-glass resistive plate chambers developing the so-called hybrid resistive plate chambers. The beam test results manifestly show the contribution of the secondary emission layer on the overall electron multiplication in the gas gap. The measurements also enable preliminary assessment of the secondary emission principle in thin Al_2O_3 and TiO_2 layers in a particle shower/avalanche environment and the development of Monte Carlo simulations. Here we describe the details of the direct utilization of the secondary electron emission surfaces and the impact of the findings on future implementations.

1 Introduction

The secondary emission (SE) principle is a fundamental concept in the operation of certain types of particle detectors. It refers to the phenomenon where primary particles (such as electrons or ions) striking a material cause the ejection of secondary particles, which can then be detected. This principle is utilized in various detector technologies to measure and analyze the properties of incoming particles.

The number of secondary electrons emitted per incident primary particle is known as the secondary emission yield. This yield depends on factors such as the energy and type of the primary particle, the angle of incidence, and the properties of the target material. The efficiency of energy transfer from the primary particle to the target atoms determines the secondary emission yield. Materials with lower work functions or those that can efficiently transfer energy from the primary particle to the electrons are more effective at secondary emission. The depth from which secondary electrons can escape to the surface without losing energy is also critically important imposing constraints on the overall thickness of the secondary emission layer.

In this report, we describe the development of detector modules working with the principle of secondary electron emission, and the implementation of secondary emission layers in gaseous detectors; and we discuss possible future implementations.

2 SE Module Development and Testing

Photomultiplier tubes (PMTs), which utilize the secondary emission principle to amplify the signal generated by incident photons, are widely used in particle detectors for their high sensitivity and fast response. In terms of SE electron generation, the SE sensor cathode functions similarly to the photocathode in a PMT. SE electrons generated at the surface by traversing shower particles, as well

*e-mail: burak.bilki@cern.ch

as those produced at the dynodes, are akin to photoelectrons [1, 2]. The electron multiplication process can utilize metal meshes or other planar dynode structures. Figure 1 illustrates a Hamamatsu [3] PMT featuring a mesh dynode structure, including a diagram of electron multiplication within the dynode chain (top); and a picture and a sketch of a Hamamatsu PMT with etched metal sheet dynodes (bottom).

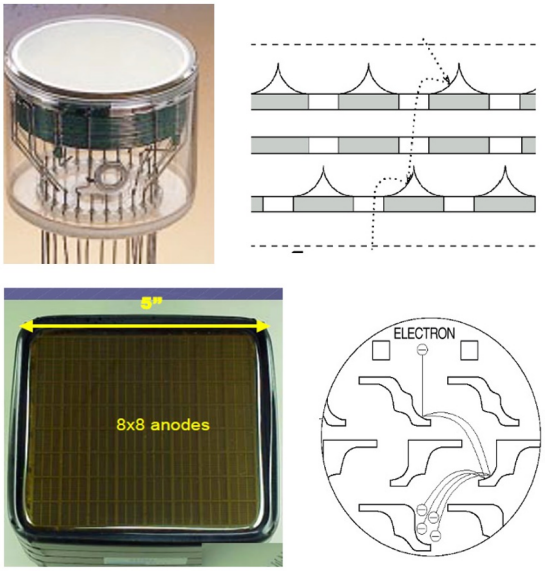

Figure 1. Pictures of Hamamatsu PMTs and sketches of mesh (top) and etched metal sheet (bottom) dynode structures.

A feasible and cost-effective SE sensor module prototype can be constructed using an array of PMTs, modified so that the photoelectron generation is disabled, utilizing only the dynode chain of the PMTs. The first SE sensor module prototypes were built with seven Hamamatsu single anode R7761 PMTs, and nine Hamamatsu R5900-00-M16 PMTs, and were extensively tested at the Fermilab Test Beam Facility (FTBF) [4] with 8 and 16 GeV electron beams. The characterization of the PMTs for this initial SE sensor module is detailed in [5]. Figure 2 shows a picture of the SE sensor module prototypes. The baseboards for both modules support three different modes of operation. In Mode 1, known as the normal divider mode, the photomultiplier voltage divider chain remains unmodified, maintaining nominal potential differences across the dynodes following Hamamatsu reference design. In Mode 2, the cathode and the first dynode are shorted. Mode 3, known as the cathode float mode, allows the cathode to be separated from the rest of the divider chain and powered by a separate high voltage source or grounded. Mode 2 was the default operation mode for the beam tests.

The lateral coverage provided by the SE module did not produce a shower signal with consistent scaling relative to shower depth when using steel absorbers. Therefore, tungsten absorbers were adopted as the baseline for subsequent tests and only one of the SE sensors were utilized downstream variable number of 1 X_0 tungsten absorbers of lateral size 50 mm x 50 mm. The trigger

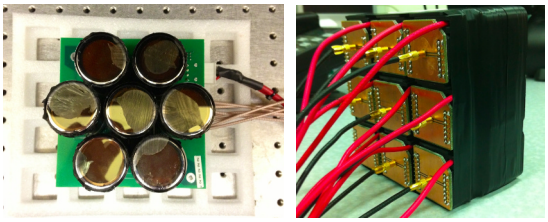

Figure 2. Pictures of the SE sensor module prototypes with mesh (left) and etched metal sheet (right) dynode structures.

counters were sized to match the sensor, and event selection was based on the beam positions measured by upstream wire chambers, resulting in precise electromagnetic shower profiles. The measurements and the Monte Carlo (MC) simulation results for the SE module with mesh dynode structure were reported elsewhere [6] and show that the electromagnetic showers are sampled sufficiently accurately and are reproduced by MC successfuly, validating the principle of secondary emission calorimetry. Figure 3 shows the 8 GeV and 16 GeV electromagnetic shower development measured with the SE module utilizing etched metal sheet dynode structure. The active area is 16 mm x 16 mm and the sensor was operated at the cathode – first dynode shorted mode. The shower shapes were fit to $A\frac{(X+X_0^U)^{(a-1)}e^{-b(X+X_0^U)}}{\Gamma(a)}$ where X is the depth of the shower in unites of radiation lengths; X_0^U is the upstream material amount in units of radiation lengths; a, b and A are free parameters. The upstream material amount was kept common for the two fits and was obtained as 1.62 X_0. The shape function describes the shower development relatively well given the size of the active area and the resulting large fluctuations in the response.

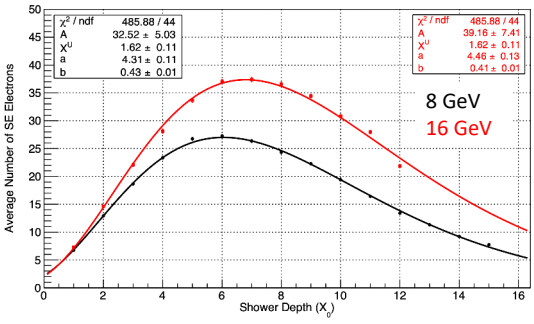

Figure 3. The 8 GeV and 16 GeV electromagnetic shower development measured with the SE module utilizing etched metal sheet dynode structure.

The electron multiplication in the SE cathode and dynodes can be enhanced by applying thin film coatings of materials with high secondary electron emission yields, such as Al_2O_3, SnO_2, TiO_2, or ZrO_2. MC studies indicate that Al_2O_3 shows the best performance at around 100 nm thickness among the above list in the thickness range of 10 nm - 5 μm. The secondary electron emission efficiency ranges between 2% and 5% for all the simulated secondary

emitter coatings were obtained. The simulations also predict a secondary electron yield of around 68 for a 100-nm Al_2O_3-coated copper foil.

A simulation study for a large-scale SE calorimeter system was conducted, modeling the SE sensor modules as 9-stage dynode chains. The dynodes were spaced 150 μm apart and featured holes with diameters of 10-100 μm, spaced 50-100 μm apart. For events where minimum ionizing particles produced an SE electron at the cathode, the average charge per SE sensor module was found to be 300 fC. The electromagnetic response of a sampling calorimeter with 16 SE modules interleaved with 1 X_0 tungsten absorbers was simulated for 1-32 GeV electrons, reflecting the typical energies at FTBF, and an electromagnetic energy resolution of $16.7\%/\sqrt{E}$ was predicted.

3 Utilization of Secondary Emission Principle in Gaseous Detectors

Recently, we applied high secondary emission yield materials, Al_2O_3 and TiO_2, as surface coatings on the anode plates of one-glass Resistive Plate Chambers (RPCs), creating the so-called "hybrid RPCs". We built several 10 cm x 10 cm x 1.3 mm (gas gap) chambers with single pad readout. Coating of Al_2O_3 was made with magnetron sputtering at Gazi University Photonics Application and Research Center [7]. Coating of TiO_2 was made with air-brushing after dissolving TiO_2 in ethanol. Figure 4 shows pictures of the anode plate before (left) and after (right) TiO_2 coating.

Figure 4. Pictures of the anode plate before (left) and after (right) TiO_2 coating.

We tested the first-generation hybrid RPCs as well as the standard 1-glass and 2-glass RPCs at Fermilab test beam. The gas mixture was the CALICE [8] DHCAL [9] RPC gas mixture R134A : Isobutane : SF6 ; 94.5 : 5.0 : 0.5 at 2-3 cc/min flow rate, approximately half of the nominal value of 5 cc/min. The hybrid RPCs with 350 nm and 500 nm Al_2O_3-coated anodes and 0.5 mg/cm^2 and 1 mg/cm^2 TiO_2-coated anodes outperformed the standard RPCs in terms of the high voltage threshold at which the chambers exceed 90% efficiency. This threshold is around 8.5 kV for the standard 2-glass RPC, 7.5 kV for the standard 1-glass RPC and 6.5 kV for the hybrid RPCs. These tests validate the charge multiplication in the secondary emission layer [10].

The hybrid RPCs with segmented readout of their anodes were constructed and tested at FTBF in a second test campaign. The purpose was to study the spatial and timing properties of the various SE coatings in detail. Due to accelerator problems, the measurements were performed with limited statistics. Also due to the limited number of readout channels, a special assembly was made: A pin board was designed to make contacts to the 1 cm^2 pads in a readout area of 8 x 8 pads. An adapter board was designed to combine the signals of several pads into a single readout channel. The pin board and the particular combination scheme for five readout channels is shown in Fig. 5 (top), and a picture of the adapter board testing is shown in Fig. 5 (bottom).

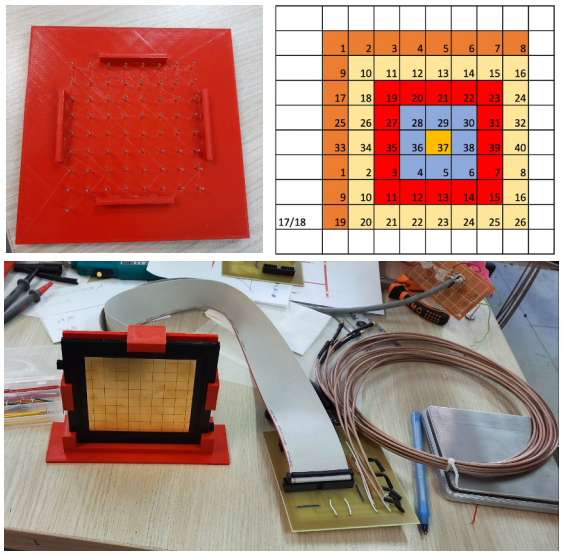

Figure 5. The picture of the pin board and the schematic of the 64-to-5 readout scheme (top) and a picture from the adapter board test station (bottom).

Figure 6 shows the average avalanche charge as a function of the wire chamber coordinates for the outermost L-shaped readout area. The boundary of the readout area is visible despite the very low statistics.

Recently, to be used as the beam loss monitoring system at the Turkish Accelerator and Radiation Laboratory [11], we developed hybrid drift tubes where the 127 μm diameter nichrome wire is coated with TiO_2/Al_2O_3 and is used as the central electrode at the center of a 10 mm inner-diameter stainless steel tube. TiO_2 coating was done by dipping the wire in the TiO_2-ethanol solution and letting the ethanol evaporate. Microscopic observation yields better than 90% coating coverage with relatively good uniformity of the coating. Al_2O_3 coating was done with magnetron sputtering and approximately 40% coating coverage was obtained with the current wire rotation system. Figure 7 (top) shows a picture of the hybrid drift tubes constructed with different anode wire coating parameters and Fig. 7 (bottom) shows an oscilloscope image from the preliminary tests performed with cosmic rays (this picture)

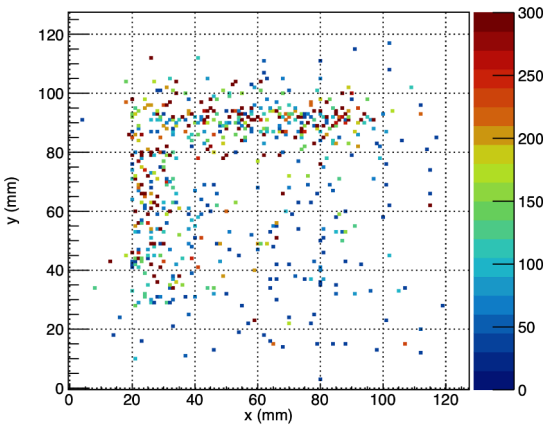

Figure 6. The average avalanche charge as a function of the wire chamber coordinates for the outermost L-shaped readout area of the high segmentation hybrid RPC.

and ^{137}Cs radioactive source. The hybrid drift tubes will be extensively tested in the laboratory for performance stability before being installed in their final locations.

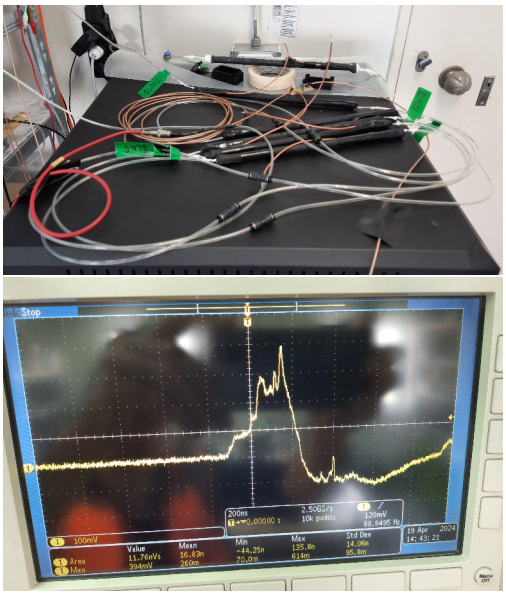

Figure 7. A picture of the hybrid drift tubes constructed with different anode wire coating parameters (top) and an oscilloscope image from the preliminary performance tests with cosmic rays (bottom).

4 Conclusions

The secondary electron emission principle offers significant potential for advancing both new and existing particle detectors:

- High secondary electron emission yield materials can be easily applied on various surfaces in the laboratory; and facilities that can apply them in much larger areas exist.
- Secondary emission calorimetry is particularly advantageous for electromagnetic calorimetry, especially in high radiation environments. The enhanced electron multiplication capability of secondary emission materials allows for more precise energy measurement and better detection of electromagnetic showers. This principle is also applicable to other areas such as beam loss monitors and Compton polarimeters, where accurate detection and measurement are crucial.
- The construction of dedicated secondary emission sensor modules is straightforward. These modules are designed to be compact, robust, and cost-effective, making them accessible for various research and industrial applications.
- Initial tests validate the effectiveness of secondary electron emission materials in different detector types. These tests confirm that the materials provide significant improvements in performance, supporting their use in future detector designs.
- Highly segmented readout for imaging calorimetry with secondary emission sensors is possible.

B. Bilki acknowledges support under Tübitak grant no: 123F335 for the development of the hybrid drift tubes.

References

[1] D. Winn et al., "Secondary Emission Calorimeter Sensor Development", Journal of Physics: Conference Series 404, 012021, 2012.
[2] F. Ozok et al., "Geant4 simulation of a conceptual calorimeter based on secondary electron emission", JINST 12 P07014, 2017.
[3] www.hamamatsu.com
[4] https://ftbf.fnal.gov/
[5] E. Tiras et al., "Characterization of photomultiplier tubes in a novel operation mode for Secondary Emission Ionization Calorimetry", JINST 11, P10004, 2016.
[6] B. Bilki et al., "Secondary Emission Calorimetry", Instruments 2022, 6, 48. https://doi.org/10.3390/instruments6040048
[7] https://fotonik.gazi.edu.tr
[8] https://twiki.cern.ch/twiki/bin/view/CALICE/WebHome
[9] C. Adams et al., "Design, construction and commissioning of the Digital Hadron Calorimeter - DHCAL", JINST 11, P07007, 2016.
[10] M. Tosun et al., "Development of hybrid resistive plate chambers", Nucl. Instrum. and Meth. A 1054, 168448, 2023.
[11] https://tarla-fel.org/